Uncertainty analysis and validation of the estimation of effective hydraulic properties.

Arnaud Mesgouez, Samuel Buis, Stéphane Ruy, Gaëlle Lefeuve-Mesgouez

Uncertainty analysis and validation of the estimation of effective hydraulic properties

A. Mesgouez,[1,2] S. Buis,[2,1] S. Ruy,[2,1] G. Lefeuve-Mesgouez,[1,2]

S. Buis, INRA, UMR1114 EMMAH, F-84914 Avignon, France (sbuis@avignon.inra.fr)

G. Lefeuve-Mesgouez, Université d'Avignon et des Pays de Vaucluse, UMR1114 EMMAH, Faculté des Sciences, F-84000 Avignon, France (gaelle.mesgouez@univ-avignon.fr)

A. Mesgouez, Université d'Avignon et des Pays de Vaucluse, UMR1114 EMMAH, Faculté des Sciences, F-84000 Avignon, France (arnaud.mesgouez@univ-avignon.fr)

S. Ruy, INRA, UMR1114 EMMAH, F-84914 Avignon, France (ruy@avignon.inra.fr)

[1]Université d'Avignon et des Pays de Vaucluse, UMR1114 EMMAH, Faculté des Sciences, F-84000 Avignon, France.

[2]INRA, UMR1114 EMMAH, F-84914 Avignon, France.

Abstract.

The determination of the hydraulic properties of heterogeneous soils or porous media remains challenging. In the present study, we focused on determining the effective properties of heterogeneous porous media with an analysis of the uncertainties at the Darcy scale.

Preliminary, experimental measurements of the hydraulic properties of each component of the heteregeneous medium were obtained. The properties of the effective medium, representing an equivalent homogeneous material, had been determined numerically by simulating a water flow in a 3D representation of the heteregeneous medium, under steady-state scenarios, using its components properties. One of the major aspects of this study was to take into account the uncertainties of these properties in the computation and evaluation of the effective properties. This was done using a bootstrap method.

Numerical evaporation experiments were conducted both on the heterogeneous and on the effective homogeneous materials to evaluate the effectiveness of this upscaling approach. First, the impact of the uncertainties of the component properties on the simulated water matric potential was found to be high for the heterogeneous material configuration. Second, it was shown that the use of the upscaling method led to a reduction of this impact. Finally, the adequacy between the means of the simulations for the two configurations confirmed the suitability of the upscaling approach used, even in the case of dynamic scenarios.

The methodology proposed in this study is generic. It was applied here to green roof substrates, a two-component media composed of bark compost and pozzolan, used in the construction of buildings.

1. Introduction

When considering vadoze zone science and hydrology science, heteregeneous media can be assessed at three different scales at least, following *Renard et al.* [1997], *Feyen et al.* [1998], *Vogel and Roth* [2003] or *Vereecken et al.* [2007]. The first scale of interest (or microscopic scale) is that of individual pores, in which water flow through the heterogeneous porous media is described by the Navier-Stokes equations. In this case, spatial variability arises from variations in pore-sizes and pore wall properties across characteristic lengths of a few micrometers. The second scale of interest from a decision making point of view is the field scale, for which the subscale heterogeneity such as spatial distribution of homogeneous units and/or spatial variability of properties are not taken into account. The third scale of interest (or macroscopic scale) is this intermediate scale, the characteristic length of which ranges from centimeters to decimeters. This is the scale at which hydraulic parameters are meaningfull and can be measured. It is usually called the Darcy scale for hydraulic properties. The work presented in this manuscript was conducted at this scale.

At the Darcy scale, heterogeneous medium can be represented in different ways. A detailed description of the various representations can be found in the reviews of *Renard et al.* [1997] or *Vereecken et al.* [2007]. Basically, the heterogeneous medium can be modeled with a spatial distribution of properties inside a single unit, see *Vogel et al.* [2010] among others, or with a patchwork of homogeneous sub-units, see *Samouëlian et al.* [2011] for example. These sub-units can be natural units defined from pedological characterisation, *Ma et al.* [2010], *Samouëlian et al.* [2011], or artificial ones that can be obtained from several calibrated sands, *Danquigny and Ackerer* [2005]. The approach proposed in this

article refered to the second way of representation and the heterogeneous material is thus modeled as a mixture of various porous media. Each component of the heteregeneous medium can be considered as a single-phase continuum, the properties of which are defined by macroscopic parameters (hydraulic conductivity and water retention curves) and by phenomenological laws (the Darcy law and the Richards equation). Water flow simulation or water balance computation can be perfomed on an elementary volume by using a numerical solver of the Richards equation accounting for the spatial heterogeneity of the hydraulic properties. The spatial structure must be known to distribute the hydraulic properties of both materials on the volume of interest. Solving the Richards equation is very tedious, in this case, since it is a non linear equation applied to multidimensional geometry. A simpler approach would be to replace the explicit three-dimensional structure of the heteregeneous volume by a homogeneous medium, the properties of which would take into account the hydraulic properties of each material, in such a way that simulations conducted on both domains would produce similar boundary water fluxes under identical boundary Dirichlet conditions, *Samouëlian et al.* [2011]. This approach would lead to equations containing fewer unknowns, and the parametrisation of which would, therefore, be easier to perform (homogeneous and uniform properties instead of heterogeneous and non-uniform properties), and which would be solved more rapidly and more efficiently. Such a medium and such properties are known, respectively, as an effective medium and effective properties.

The first objective of this study was to characterize the effective hydraulic properties of real samples taking into account uncertainties in the determination of the hydraulic properties of its individual components. Due to the recent advances in computing ca-

pabilities, numerical approaches are now widely used for the determination of effective properties, *Samouëlian et al.* [2007], *Vogel et al.* [2010]. Previous studies carried out on natural soils include *Vogel and Roth* [1998], *Javaux and Vanclooster* [2006] or *Samouëlian et al.* [2011], the authors of which estimated the effective hydraulic properties of agricultural silt soil, monolithic subsoil, or Albeluvisol, respectively, but did not integrate a complete uncertainty evaluation in their studies. However, the process of estimating the hydraulic properties of a given material include various sources of uncertainty, *Mohrath et al.* [1997], *Peters and Durner* [2008], that may significantly affect numerical simulations, *Christiaens and Feyen* [2001], *Coppola et al.* [2009], *Pan et al.* [2009], and thus affect the estimation of effective properties or their evaluation using dynamic scenarios. Therefore, estimating the resulting uncertainties on the estimation of hydraulic properties and their impacts on simulation results is important to assess the quality of effective properties estimation and to interpret the results. Taking into account all type of uncertainties using for example Monte Carlo error propagation method would be very tedious and difficult since they are numerous and since modelising their probability distribution, including possible dependancies, would be extremely complicated. The bootstrap method is a resampling method, and is recognized to be a simple and efficient way of estimating the probability distribution of a statistic. It can be used to estimate a statistic without it being biased, to evaluate the accuracy of this estimation and/or to build confidence intervals for this statistic, *Efron and Tibshirani* [1993], *Manly* [2007]. Here, we propose to evaluate the uncertainty of the hydraulic properties of the equivalent homogeneous medium by taking into account, in the numerical processing, the uncertainties estimated for the hydraulic properties of each component.

The second objective of this study was to evaluate the effectiveness of the previous upscaling approach with respect to dynamic simulations. Several authors, *Vogel et al.* [2008], *Vogel et al.* [2010], have previously noted that simulations conducted using effective parameters may differ from simulations conducted with spatially variable parameters, in particular when non-equilibrium flows are involved. An evaluation of the upscaling methodology would, therefore, be required and should be performed by minimizing the occurrence of non-equilibrium flows. In the present study, simulations of a dynamic evaporation process using either the heteregeneous medium or the effective homogeneous material were compared, as it was previously shown that non-equilibrium flows are generally absent under evaporation conditions, *Šimůnek et al.* [2001]. The comparisons were once again performed by including uncertainties estimated for the hydraulic properties of both the heteregeneous and effective homogeneous materials.

In this study, the methodology was applied to green roof substrates, hereafter called substrate or complex substrate, which is a composite of compressible materials, namely organic matter (bark compost) used as fertilizer, and of aggregates of volcanic rock (pozzolan) used as rigid skeleton. These two-component materials are considered to serve a number of beneficial purposes that can help in the management of various environmental problems, such as the reduction of air pollution or of the carbon footprints of cities, the improvement of storm water management and, of course, the improvement of energy efficiency in buildings. Several bark compost and pozzolan samples were studied and the uncertainty of their hydraulic properties were estimated.

The manuscript is structured as follows. In section 2, the material characteristics are described for the two components of the substrate, and the experimental and numerical

methodologies for obtaining the hydraulic properties as well as their associated uncertainties are stated. Section 3 presents the numerical tools used to obtain the effective hydraulic properties of the heteregeneous medium and the uncertainties associated with these properties, and to evaluate the effectiveness of the upscaling approach. In section 4, values and uncertainties obtained for the hydraulic properties of each component of the heteregeneous as well as of the effective materials are presented and discussed. Simulation results of dynamic evaporations of the two-component substrate and the effective medium are then presented to evaluate the upscaling approach. Finally, concluding remarks and future research perspectives are briefly outlined in section 5.

2. Estimation of material properties and associated uncertainties from experimental measurements

2.1. Experimental procedures

The green roof substrate under study was composed of a combination of 40% organic material (bark compost) and 60% volcanic material (pozzolan). This combination corresponds to the volumetric proportions which are actually used in an *in situ* environment. Bark compost was provided by an industrial partner and the precise composition of this compost is confidential. Pozzolan materials were extracted in a quarry located in the "Massif Central" mountain in the center of France. Chemical composition of pozzolan was given by the operator of the quarry ($SiO_2 : 42 - 55\%; Al_2O_3 : 12 - 24\%; Fe_2O_3 : 8 - 20\%$). The pozzolan grain size distribution was the following: 2/3 of the pozzolan grain diameters ranged from 3 to 6 mm, and 1/3 from 7 to 15 mm.

Estimating the hydraulic properties at the Darcy scale required the preliminary characterization of the physical and hydraulic properties of both materials under laboratory con-

ditions. The properties of the two materials were measured on samples of both materials, and were measured at the same bulk density $[M.L^{-3}]$ as they occur in the actual substrate. Since bark compost is a compressible material, contrary to pozzolan, we followed the procedure described hereafter to be certain that the density of pure bark compost samples was the same as the density of bark compost present in the actual composite substrate. The complex substrate was characterized following a standard compaction methodology, namely the Proctor compaction test, standard DIN 18127. The sample was struck 6 times by a 4.5 kg Proctor hammer from a height of 45 cm in order to obtain adequate compaction. The compacted sample obtained following this methodology, was supposed to be representative of the *in situ* industrial execution of the green roofs, *Anonymous* [2002]. By knowing, on the one hand, the apparent bulk density of the substrate and of the pozzolan aggregates and, on the other hand, the solid density of bark compost and of pozzolan, we extrapolated the apparent bulk density of bark compost in the actual composite substrate. Bark compost samples could subsequently be compacted down to this apparent bulk density and their hydraulic properties, i.e. water retention and hydraulic conductivity, could be measured using ad hoc experimental procedures for different water potentials. These hydraulic properties were then modeled for each material by fitting parametric models to these experimental data.

The experimental procedures carried out, and the methodology used to estimate the hydraulic properties and the associated uncertainties are described in the following sections.

2.2. Uncertainty evaluation methodology

Various approximations and errors can be sources of uncertainty when estimating the hydraulic properties of each material. The following typology is proposed to classify these sources of uncertainty:

1. Variability in the properties of samples: owing to the variability of the material samples used in some experiments, or to the fact that some experiments result in the destruction of the samples used, measurements of the properties of a material are often replicated using several samples. The number of samples used may have a significant impact on the estimation of the hydraulic properties of a material depending on the level of their individual variability,

2. Errors in experimental data due to (i) approximations performed on length, weight or density measurements, for instance transducer locations, and to (ii) digitalization errors associated with digital data-loggers. These errors can propagate in the estimation of the hydraulic properties as noted by *Tamari et al.* [1993],

3. Model errors due to inadequate model assumptions. *Vogel et al.* [2010] showed in a numerical case study that the validation of the upscaling process required a highly flexible hydraulic law model,

4. Fitting errors: in the event of a low number of experimental data, the level of uncertainty of the parameters obtained using parametric models fitted to the experimental data may be very high, even in case of slight variability in the properties of the samples and of slight measurement errors.

We used the bootstrap method, *Efron and Tibshirani* [1993], *Manly* [2007], to estimate the resulting uncertainties on the hydraulic properties and to evaluate their impacts on

the simulation results. This method can be used to estimate a statistic without it being biased, to evaluate the accuracy of this estimation and/or to build confidence intervals for this statistic. In the present study, the statistics computed were the parameters of the laws describing hydraulic properties. In the following, we describe the principle of non-parametric bootstrapping which is relatively simple. Let us consider the observation sample obtained for the computation of the statistic, in our case a set of water retention or conductivity measurements associated with water potential values. These observations must be independent and identically distributed to ensure the convergence of the method. N artificial samples, of the same size as the original observation sample, are created by sampling in it with replacement. They are called bootstrap samples. The statistical value is computed for each of these bootstrap samples. Its probability distribution is then approximated using the histogram of the N computed statistical values. In other words, the actual variability of the statistic is estimated using the observed variability of the whole of the samples obtained by resampling. Of course, this kind of methodology does not take into account the problem of model error, of large biases or of samples non representative of the population, although it produces accurate descriptions of uncertainties under reasonable assumptions and a lower bound of the actual uncertainty level.

2.3. Determination of solid density and apparent bulk density of compost and pozzolan

Samples were crunched, sieved at 315 μm and air dried in the oven for 24 h at 105 °C. Solid particles were then placed in the measurement chamber of a He pycnometer and solid bulk density was determined using the Boyle law, *Dane and Hopmans* [2002]. The apparent bulk density of pozzolan aggregates was measured on replicates with diameters

varying from 7 to 15 mm, using Archimede's law and buoyancy measurements in water. The aggregates were previously saturated in water for 24 h, *Monnier et al.* [1973]. The apparent bulk density of the composite substrate was measured using the core method, *Dane and Hopmans* [2002], adapted for compacted and remolded samples. The apparent bulk density of bark compost present within the composite substrate was deduced. All of the measured properties are displayed in Table 1.

2.4. Determination of water retention and associated uncertainties

Water retention measurements were obtained using the suction table for small suctions $(0.05, 0.54, 1.03, 2.01, 3.97, 6.91$ kPa) and the pressure plate extractors for large suctions $(10, 30, 50, 100, 300, 500$ and 1500 kPa), *Dane and Hopmans* [2002]. The total number of replicates differed for pozzolan and bark compost materials.

1. Since pozzolan aggregates are a natural material with a high level of variability due to geological variations occuring during their formation, a large number of replicates were required to counter the effects of this natural heterogeneity. 10 different aggregates were used for each suction point. The aggregates taken for apparent bulk density measurements were also used for the 0 kPa suction point. Water saturated aggregates were gently placed onto a fine layer of kaolinite paste to ensure a good contact between aggregate pores and the sand layer (for suction tables) or the porous plate (for pressure plate extractors). A set time for sample equilibration of 3 days was respected.

2. Bark compost samples were compacted in the laboratory following a standard procedure in order to obtain a predetermined density of compost into the composite substrate, the variability of which was very low (see Table 1). A low number of replicates were, therefore, required. 5 different bark compost samples were used for each suction point.

To account for any natural variability in the density of bark compost within the composite substrate, samples were compacted in small cylinders ranging from 0.184 and 0.213 g.cm^{-3}. Mean bulk density was 0.200 g.cm^{-3}, which differs slightly from the theoretical bulk density of compost within the composite substrate (0.195 g.cm^{-3}), due probably to experimental approximations. After initial saturation, samples were placed onto the suction table or porous plate. Kaolinite paste was also used to increase the quality of the capillary connectivity between the sample and the sand layer or porous plate. The time needed for sample equilibrium was over one week for each suction point and was controlled by monitoring the water flow out of the pressure chamber.

The van-Genuchten model, *van Genuchten* [1980], was fitted to the experimental data in order to obtain the water retention curve, i.e. the relation between $\theta(h, \mathbf{x}, t)$ $[L^3.L^{-3}]$ the volumetric water content and $h(\mathbf{x}, t)$ $[L]$ the water matric potential, as follows

$$\theta(h, \mathbf{x}, t) = \theta_r + (\theta_s - \theta_r) \times \left[1 + \left(\frac{h(\mathbf{x}, t)}{h_e}\right)^n\right]^{-m} \quad (1)$$

where $\mathbf{x}$ $[L]$ are the spatial coordinates, t $[T]$ is the time, θ_r $[L^3.L^{-3}]$ is the residual volumetric water content, θ_s $[L^3.L^{-3}]$ is the water content at saturation, $h_e[L]$ is a scale parameter, n $[-]$ and m $[-]$ are shape parameters with $m = 1 - 1/n$.

First, all the measured data were used to estimate the values of the van Genuchten model parameters for pozzolan and bark compost. Then, uncertainties of these parameters were estimated by bootstrapping measured data for each suction point. The van-Genuchten model was, thus, fitted N times, with $N = 500$ in this case, on N datasets obtained by resampling with replacement the measured data. The N resampled datasets contained the same number of measurements as the original samples, in total and for each suction

point. The van-Genuchten model fits were performed using the non-linear least squares regression taking into account measurement error variances for each suction point and using the trust-region-reflective minimizer, *Coleman* [1996].

2.5. Determination of hydraulic conductivity and associated uncertainties

Hydraulic conductivity was measured for pozzolan and bark compost under water-saturated and unsaturated conditions using two different methods. Hydraulic conductivity at saturation K_{Sat} $[L.T^{-1}]$ was measured using a constant head permeameter, *Chossat* [2005], for pozzolan cores and bark compost samples. Unsaturated hydraulic conductivity was measured using the Wind evaporation method, *Tamari et al.* [1993]. Samples used for determining the hydraulic conductivity at saturation were also used for determining the unsaturated hydraulic conductivities. As was the case for determining the water retention curve, the number of replicates differed for pozzolan and bark compost, and were adapted to the different variability of both materials: 10 replicates were used for pozzolan and 1 replicate was used for bark compost.

Samples of pozzolan were extracted from large blocks (volume of approximately 1 dm^{-3}). Initially, a classification of these blocks was made based on the visible porosity and the estimated bulk density: an equal number of "compact" and "porous" blocks in equal quantities were identified. 10 replicates were then cored from both types of blocks. The vertical walls of the clods were surrounded by heat shrink tubing to avoid preferential water flow along the walls during measurements.

Samples of bark compost were obtained after their compaction up to 0.195 $g.cm^{-3}$ in cylinders. A single replicate was used, since a low experimental variability was expected

as the compaction procedure was accurately performed and led to a very low level of variability in the porosity obtained (see Table 1).

For measuring the unsaturated hydraulic conductivity, pozzolan clods and bark compost were equipped with sufficient microtensiometers to obtain an accurate estimation of their hydraulic properties, *Tamari et al.* [1993]. After sample saturation, water was allowed to evaporate from the upper surface of each core under laboratory conditions, i.e. conditioned atmosphere at 24 °C under atmospheric pressure. The base of each core was sealed to prevent downward flux.

The Mualem-van Genuchten model, *van Genuchten* [1980], was fitted to the experimental data to obtain the hydraulic conductivity curve, i.e. the relation between $K(h, \mathbf{x}, t)$ $[L.T^{-1}]$ and $h(\mathbf{x}, t)$

$$K(h, \mathbf{x}, t) = K_{Sat}.\Theta^{0.5}(h, \mathbf{x}, t)\left[1 - (1 - \Theta^{1/m})^m\right]^2 \tag{2}$$

where

$$\Theta(h, \mathbf{x}, t) = (\theta(h, \mathbf{x}, t) - \theta_r)/(\theta_s - \theta_r) = \left[1 + \left(\frac{h(\mathbf{x}, t)}{h_e}\right)^n\right]^{-m} \tag{3}$$

As for water retention, all the measured data were first used to estimate the values of the Mualem-van Genuchten model parameters for pozzolan and bark compost. Then, uncertainties linked to the variability of the pozzolan clod properties were simulated by bootstrapping in the 10 pozzolan clods. Uncertainties linked to the experimental setup and data processing were dealt with by bootstrapping in each clod dataset. N datasets, with $N = 500$, were thus built by resampling with replacement in the 10 pozzolan samples and within each selected dataset. Since each resampling step maintained a constant dataset size, N corresponding conductivity curves were, thus, fitted using the Mualem-

van Genuchten model on these N datasets. The Mualem-van Genuchten model fits were performed using the non-linear least squares regression assuming error homoscedasticity and using the same minimizer as for the water retention fit.

Porosity ϕ of bark compost was measured for a single set of samples. The uncertainty of the measured saturated hydraulic conductivity could, thus, be estimated from the variability in the porosity values using the Kozeny-Carman model, *Kutilek and Nielsen* [1994]. A simple error propagation computed using this model, assuming a log-normal distribution of K_{Sat}, gave rise to

$$\mathrm{var}\left[\log(K_{Sat})\right] = \left(\frac{3-\phi}{\phi(1-\phi)}\right)^2 \mathrm{var}(\phi) \tag{4}$$

An approximation of the probability distribution of the hydraulic conductivity of compost was computed by fitting the Mualem-van Genuchten model to $N = 500$ datasets built by bootstrapping in the experimental dataset. Each one of the N datasets also included a single value for K_{Sat} randomly sampled from the uncertainty distribution estimated as described above. The regression was performed using the same assumptions and methods as for the regression measured for the hydraulic conductivity of pozzolan.

3. Computation of effective hydraulic parameters

Effective hydraulic parameters were determined by numerically simulating a water flow, under specific conditions, in a three-dimensional representation of the heterogeneous material. This required the preliminary solving of the highly non-linear Richards equation (RE). Simulations were performed herein with a specific C++ parallelized code.

3.1. C++ parallelized code and simulation configuration

The three-dimensional variably saturated flow modeling was based on the non-linear Richards equation. The mixed form of RE obtained by combining the mass conservation law with the generalized Darcy equation was

$$\frac{\partial\theta(h,\mathbf{x},t)}{\partial t} = \nabla.\left(K(h,\mathbf{x},t)\nabla(h(\mathbf{x},t)+z)\right) + Q(\mathbf{x},t) \tag{5}$$

where z is the upward vertical coordinate and $Q(\mathbf{x},t)$ is a sink or/and source term. Constitutive functions depending on the materials considered link $h(\mathbf{x},t), \theta(h,\mathbf{x},t)$ and $K(h,\mathbf{x},t)$ and close (5). Various initial and boundary conditions can complete the parabolic system of partial differential equations.

Water flow was solved using the mixed form of the Richards equation for which a perfect mass balance is ensured, see *Celia et al.* [1990], *Kavetski et al.* [2001], *Renaud et al.* [2003] to cite a few. Spatial discretization was performed using the Galerkin-type linear isoparametric finite elements, *Dhatt et al.* [1984], *Ju and Kung* [1997]. The modified Picard iteration scheme was implemented in a fully implicit Euler time discretization. Different convergence criterion could be used, as explained in *Huang et al.* [1996]. An adaptive time step adjustment was implemented to improve numerical efficiency, *Kavetski et al.* [2001]. Time and spatial discretizations resulted in the following system of linear equations

$$\left[\frac{[M^{t+1,m}][C^{t+1,m}]}{\Delta t} + [K^{t+1,m}]\right]\{\delta_u^m\} =$$
$$\{F^{t+1,m}\} - \frac{[M^{t+1,m}]}{\Delta t}\{\theta^{t+1,m}\} + \frac{[M^{t+1,m}]}{\Delta t}\{\theta^t\} - [K^{t+1,m}]\{u^{t+1,m}\} \tag{6}$$

where t and m denote, respectively, time and inner iteration levels, $u = h + z$ and $\delta_u^m = u^{t+1,m+1} - u^{t+1,m}$, $[M]$ and $[K]$ are the global mass and stiffness matrixes, F includes the source/sink terms and $[C(h,\mathbf{x},t)]$ is the specific moisture capacity function matrix.

A C++ object oriented code was developed to solve (6) and to determine the water matric potential and the water flux at each node/boundary of the finite element mesh grid for an unsaturated medium. Our numerical results were found to corroborate analytical results published by *Fityus and Smith* [2001], *Tracy* [2007] or purely numerical results proposed by *Vanderborght et al.* [2005].

Due to the specific composition of the green roof substrate, very fine spatial grids were required, leading to huge CPU time and storage cost. This major drawback was overcome by a parallelization of the code, *Hardelauf et al.* [2007], *Herbst et al.* [2008]. MPI (http://www.mpi-forum.org/) and PETSc (http://www.mcs.anl.gov/petsc/) libraries were used herein to parallelize the C++ sequential code.

Numerical simulations were performed on a typical soil core to compute the effective parameters at the Darcy scale. In our case, the green roof substrate was represented by a cylinder of the following dimensions: height = 7 cm and diameter = 15 cm. This cylinder was discretized with $507,553$ nodes and $3,216,152$ elements. The average length of each edge was approximately 1.5 mm. As mentioned above, the pozzolan grain size distribution was the following: 2/3 of the pozzolan grain diameters ranged from 3 to 6 mm, and 1/3 from 7 to 15 mm. A specific algorithm was developed to model the geometry and distribution of pozzolan. This algorithm took into account a mesh of the cylinder obtained by GMSH (http://geuz.org/gmsh/). Grains of pozzolan were then created by randomly selecting a seed represented by an element of the mesh. The volume of the grain was randomly chosen from the known grain diameter distribution and assumed that the pozzolan grains were spheric. The grains were then iteratively built by randomly selecting

and aggregating adjacent elements of the growing irregular seeds until the required grain volumes were reached. Fig. 1 shows a typical mesh used in the simulations.

3.2. Computation of effective parameters and associated uncertainties

The effective parameters were obtained using a steady-state flow simulation, as explained in *Samouëlian et al.* [2007] or *Samouëlian et al.* [2011], in the interval $[-10^2, -10^{-2}]$ m, which corresponds to the validity range of the numerical code. The same water matric potential, a Dirichlet type condition, was applied to the upper and the lower boundaries of the cylinder, leading to a constant water matric potential throughout the medium in the case of a homogeneous material. The vertical boundaries were impermeable. In order to obtain the hydraulic conductivity, the calculated water flux was divided by the surface of the upper boundary. In the case of a heterogeneous medium, the same configuration led to an almost constant water matric potential in the medium, and the so-called effective hydraulic conductivity of the composite substrate was equal to the average water flux density across the horizontal boundaries. The water retention was calculated for each element with the computed values of nodal matric potential. These conductivity and water retention values were relative to the matric potential value fixed at the boundaries, even if local gradients of matric potential were present within the heterogeneous medium. The computation was, thus, repeated for several water matric potential values in order to fit the conductivity and retention curves. For each water matric potential value relative to the boundary conditions, the following question arose: how to be "sure" that the steady-state flow was reached? The lower water flux was compared to the upper flux and both were calculated at each time point. When relative differences *i*) between two successive time iterations for each water flux and *ii*) at time t between the upper and lower flux

354 became lower than $\epsilon/10$, where ϵ was the required precision of the inner iteration scheme,
355 the simulation was stopped. $\epsilon = 1e-4$ was used here.

356 In order to take into account uncertainties in the hydraulic properties of pozzolan and
357 compost, the computation of the effective hydraulic conductivity and water retention for
358 each water matric potential value was repeated for a single set of pozzolan and compost
359 properties randomly sampled from their uncertainty distributions. The spatial distribu-
360 tion of the pozzolan grains in the mesh was different for each repetition and was generated
361 randomly as explained above. The sampling of pozzolan and compost properties was per-
362 formed independently for each water matric potential value. The choice of the number
363 and values of water matric potential points and the number of replicates for each water
364 matric potential value, directly affected the computational cost of the estimation of the
365 effective properties and their level of uncertainty. An optimal experimental design tech-
366 nique was used to guide these choices. A D-optimal criterion, *Atkinson and Doney* [1992],
367 was computed for fitting the Mualem-van Genuchten and the van Genuchten models. The
368 aim was to minimize this D-criterion which is the determinant of the error covariance ma-
369 trices of the models parameters. Several contrasted water matric potential distributions
370 of points were considered in the bounded interval $[-10^2, -10^{-2}]$ m : regular distribution,
371 log-regular distribution and quantiles of beta distributions to concentrate points on the
372 left, the right or the center of the interval. The log-regular distribution appeared to be
373 the best compromise with respect to the criterion values computed for both models for
374 a number of water matric potential values. Then, an optimisation of the ratio between
375 the number of water matric potential points and the number of replicates, for a given
376 computational cost corresponding to 200 simulations, was computed with this log-regular

distribution. In the end, the D-optimal design, among those tested, was a log-regular repartition of 4 water matric potential points with 50 replicates.

Similarly to what was done for estimating individual materials properties, all the measured data were first used to estimate the effective material properties. Uncertainty distributions of the effective properties were then obtained by bootstrapping the data computed for all replicates within each water matric potential values and fitting the Mualem-van Genuchten and van Genuchten models to each of these $N = 500$ resampled datasets. The fits were performed using the non-linear least squares regression by taking into account the measured error variances computed for each water matric potential value and using the minimizer described in section 2.4. For the Mualem-van Genuchten model fit, prior information on K_{sat} was considered to regularize the fitting problem. This prior information was modeled as a bounded gaussian distribution. Its bounds were defined as the minimum and maximum of the theoretical Wiener bounds (see section 4.2) at 0 m water matric potential value. Its mean was set to the middle of this interval and its standard deviation to the quarter of its length.

3.3. Evaluation of the upscaling approach under dynamic evaporation

Reliability and accuracy of the estimation procedure of the effective parameters were evaluated using dynamic scenarios. Our aim, here, was to cross-check the upscaling and the bimaterial approaches by simulating the evolution of water matric potential versus time, for various points of the soil core described in section 3.1. A time-variable flux of evaporation ranging from 1.9 mm.d^{-1} to 0.9 mm.d^{-1} was applied to the top surface of the soil core at $z = 0$. The values of the time-variable flux were representative for usual experimental conditions of the Wind evaporation method. The other boundaries

were impermeable. The initial condition was that of a quasi-saturated medium with $h(\mathbf{x}, t = 0) = -9.5$ cm for all depths. For $h = -100$ m, the flux type boundary conditions were switched to the Dirichlet conditions. The simulations lasted 10 days to ensure a greater evaporation and a switch from flux to the Dirichlet conditions at the boundary of the upper part of the soil core.

200 simulations were performed for the bimaterial configuration and for the equivalent homogeneous material, by randomly sampling the corresponding hydraulic properties in their uncertainty distributions. For the bimaterial configuration, a different spatial distribution of the pozzolan grains in the mesh was randomly generated for each simulation. For each simulation, 4 sets of 5 points were considered at 4 different depths in order to monitor the matric potentials. The vertical coordinates were: $z = 0$ cm, $z = -0.2$ cm, $z = -1.1$ cm and $z = -4.8$ cm. For each depth, the arithmetic mean values of matric potential were computed on the 5 points. The distribution of these mean values obtained for the bimaterial configuration were then compared to the distribution obtained for the equivalent homogeneous configuration at each depth.

4. Results and discussion

4.1. Water retention and hydraulic conductivity curves of pozzolan and compost

The resulting uncertainty distributions of the water retention for pozzolan and compost are presented in Figs. 2. The estimated values of the van Genuchten model parameters for compost and pozzolan and the standard deviations of the associated uncertainty distributions are displayed in Table 2.

418 The resulting uncertainty distributions of the hydraulic conductivity for pozzolan and
419 compost are presented in Figs. 3. The estimated values of the Mualem-van Genuchten
420 model parameters for compost and pozzolan and the standard deviations of the associated
421 uncertainty distributions are displayed in Table 3.

422 **4.1.1. Comments on the water retention results**

423 The water retention measurements of pozzolan were widely spread near saturation.
424 High standard deviations for water content, 0.13 m^3/m^3 to 0.14 m^3/m^3, were obtained
425 for matric potential values greater than -10^{-2} m. These decreased to a typical value
426 of 0.03 m^3/m^3 in the central part of the water retention curve and were under 0.007
427 m^3/m^3 for the lowest ($h < -10$ m) matric potential values. According to the Jurin law,
428 water content near saturation is determined by the proportion of larger pores (up to 1
429 mm in diameter) that can be found in pozzolan aggregates. Due to the small size of
430 the aggregates (diameter of about 5 mm) used in the present study, the proportion of
431 macropores was highly variable from one aggregate to the other, which explains the high
432 variability of the water content near saturation. For lower matric potential values, the
433 water content variability of pozzolan aggregates may be attributed to factors involved in
434 pozzolan formation. Indeed, pozzolan is a porous siliceous pyroclastic rock, the porosity of
435 which is created by dissolved gas entrapped in lava during scoria emission. The mineralogy
436 of rocks, the proportion of dissolved gas and the temperature of scoria during volcanic
437 eruption, all affect upon the porosity and pore size distribution of pozzolan rocks.

438 Experimental data were less spread out for the water retention of bark compost. Con-
439 trary to pozzolan, the water retention measurements for bark compost were obtained on
440 remolded, compacted samples. The porosity of compacted bark compost includes both

the matric porosity of individual bark fragments and the structural porosity between bark fragments. As observed for natural soils, *Dexter et al.* [2008], water retention near saturation was related to structural porosity. We found a very good linear relationship between water retention data and apparent bulk density for matric potentials greater than -0.7 m (data not shown). Consequently, variability in the water retention measurements was very low near saturation, since the apparent bulk density of bark compost samples was accurately controlled. For lower matric potential values, the variability was due to the variability of matric porosity and pore size distribution of bark fragments. This experimental dispersion was relatively low, since the highest standard deviation value was 0.02 m^3/m^3.

Figs. 2 show that in all the cases studied, the van Genuchten model adequately fitted water retention experimental data. The estimated uncertainty distributions had a similar behaviour to those of the experimental ones: a lower level of uncertainty for compost than for pozzolan, particularly for matric potentials between -0.01 m and -1 m, and a higher level of uncertainty near saturation. The higher level of uncertainty in the water retention values for compost near saturation was not due to greater experimental uncertainties, as was the case for pozzolan, but due to a lack of experimental data. For both materials, the most variable and least variable parameter, respectively, were h_e and the n exponent, with respective coefficient of variations of approximately 20% and 1 % for bark compost data, and 35% and 1 % for pozzolan aggregates data (see Table 2). The h_e parameter is a scale parameter which is related to the entry point of air into the studied material, whereas the n parameter is a shape parameter related to the pore size distribution, *Kutilek and Nielsen* [1994]: a greater scattering of the h_e parameter could, thus, be linked to the

macroporosity variability. A slight variability in the exponent n was representative of a homogeneous meso- and micro-pore size distribution for both materials.

4.1.2. Comments on the hydraulic conductivity results

The K_{Sat} experimental values ranged from 10^{-7} to 10^{-3} m.s^{-1} for pozzolan samples. The conductivities at saturation of "porous" blocks were higher than those of "dense" blocks (not shown here). The relative standard deviation of K_{Sat} was relatively low for compost. This was expected as was previously explained in section 2.5, and substantiated the fact that only a single sample was used for determining of the hydraulic properties of bark compost. For the unsaturated part of the hydraulic conductivity curve, the experimental scattering of (K, h) data found for pozzolan and bark compost materials were similar to the scattering of data found for natural soils using the Wind evaporation method, *Tamari et al.* [1993]. In Figs. 3, data obtained for pozzolan samples are represented with the same symbol since experimental scattering largely overlaps from one sample to the other. We observed a lack of experimental values between the data obtained under saturated and unsaturated conditions. This is due to the limited accuracy of matric potential sensors and to the Wind evaporation method: it is necessary to have significant matric potential gradients between two successive sensors to compute an accurate value of the unsaturated hydraulic conductivity, and this is usually not achieved close to saturation, *Tamari et al.* [1993]. Despite this limitation, direct computation of K values could be obtained using the Wind evaporation, which is not the case for inverse methods used either in the onestep or the multistep outflow methods, *Hopmans et al.* [2002], where only curve parameters are fitted.

Figs. 3 show that, as expected, the estimated uncertainty of the hydraulic conductivity of pozzolan was greater than that of bark compost. The uncertainty distribution of parameter n was very low for both materials (see Table 3). For the h_e and K_{sat} parameters, the scattering was greater for pozzolan material than for bark compost material.

4.2. Effective water retention and hydraulic conductivity curves

Various analytical bounds or estimations for effective hydraulic conductivities can be found in the literature, *Matheron* [1967], *Renard et al.* [1997]. The Wiener bounds give a fundamental inequality which is always valid. Let $\mu_{a|K}$ and $\mu_{h|K}$ be the arithmetic and harmonic means of conductivity values, ω_C and ω_P the volumic proportion of each material, and K_C and K_P the hydraulic conductivities of compost and pozzolan, respectively. For each water matric potential h, the effective conductivity K_{eff} can be bounded as follows

$$\mu_{h|K} = \frac{1}{\omega_C/K_C + \omega_P/K_P} \leq K_{eff} \leq \mu_{a|K} = \omega_C K_C + \omega_P K_P$$

Note that the Wiener bounds presuppose a plane layered structure of the medium. The harmonic and arithmetic means are obtained, respectively, when the water flux is perpendicular or parallel to the main orientation of the layered surface. For a statistically homogeneous and isotropic medium, *Matheron* [1967] proposed an estimation of the effective conductivity calculated by a geometric weighted average of the arithmetic and harmonic means $\mu_{a|K}$ and $\mu_{h|K}$. This curve, designed as the Matheron curve in the following sections, is defined by $\mu_{M|K} = \mu_{a|K}^{\alpha}\mu_{h|K}^{1-\alpha}$, where $\alpha = (D-1)/D$ and D is the dimension of the problem.

For effective water retention, an analytical estimation was simply obtained by the addition of the water retention properties for each component, taking into account their respective proportions.

Figs. 4 show the means and standard deviations of effective conductivity values obtained as described in section 3.2, as well as the means of the corresponding Wiener bounds and Matheron estimations. The means of the effective conductivity values, for each water matric potential value, must be included into the means of the corresponding Wiener bounds. The crosses which can be observed in Figs. 4 are well-bounded, validating the numerical procedure developed to determine the effective values. Note that the means of the effective conductivity values are closer to the arithmetic mean curve. They are above the Matheron mean curve before the intersection between the Wiener curves, and below after that intersection. Fig. 5 presents the means and standard deviations of the effective retention values. The effective water retention values computed correspond to the arithmetic mean curve. This result was already obtained by several authors, see *Samouëlian et al.* [2007], *Vogel et al.* [2008] or *Samouëlian et al.* [2011] among others. Under quasi static conditions and without dynamic effects, the water retention curve presents a capacitive property, *Vogel et al.* [2008], and the effective water retention curve can be calculated from the additive properties of the local water retention curves, *Samouëlian et al.* [2007]. The standard deviations of the effective conductivity and retention values computed for the four water potential values were between those obtained for bark compost and pozzolan, and close to the standard deviation of their arithmetic means (results not shown).

The uncertainty distributions of the effective water retention and the hydraulic conductivity are presented in Figs. 6. Estimated values and standard deviations for the corresponding parameters of the van Genuchten and Mualem-van Genuchten models are diplayed in Tables 2 and 3.

The estimated uncertainties for the effective conductivity and water retention parameters were relatively low and generally inferior to those of bark compost and pozzolan, under unsaturated conditions. This was mainly due to the size (number of replicates $\times$ number of water potential values), and to a lower extent, given this size, to the optimal choice of the numerical experimental design used for computing the effective conductivity and water retention values from those measured for bark compost and pozzolan. These uncertainties increased closer to saturation following the same trend as the one observed for individual components. The standard deviations of most of the van Genuchten and Mualem-van Genuchten parameters estimated for the effective material were lower than the ones estimated for bark compost and pozzolan. The standard deviations of the parameters, directly linked to saturated conditions (K_{Sat} and θ_s) estimated for the effective material, were between those estimated for bark compost and pozzolan. To conclude this section, the proposed methodology applied using an optimal sampling design led to "well defined" effective properties. This means that (i) the effective properties of the composite substrate could be calculated from the properties of each material and their relative proportion in the composite substrate, and that (ii) the uncertainties of the effective properties were lower than the uncertainties of the properties of each material. The reduction in the level of uncertainty was more pronounced for the van Genuchten parameters asso-

ciated to the dry part of the properties (θ_r,h_e,n) than for the ones associated to the wet part of the properties (θ_s,K_{sat}).

4.3. Evaluation of the upscaling approach under dynamic evaporation

Three snapshots of water potential values obtained at different simulation time points during the evaporation process are presented in Figs. 7 for the bimaterial configuration. Heterogeneous spatial distributions of these values were observed at the upper surface of the soil core at $t = 2$ days and $t = 6$ days. Blue shades represent the gradients due to the geometrical distribution of the two materials. Consequently, isovalues of h did not correspond to horizontal planes. At $t = 10$ days, the Dirichlet condition replaced the flux condition at the upper surface, which led to a uniform spatial distribution of water matric potential values at $z = 0$. A gradually stronger vertical gradient could be seen in-depth as evaporation took place.

Figs. 8 present the uncertainty distributions of water matric potential mean values per depths for the evaporation process and for the bimaterial configuration and the corresponding effective homogeneous material configuration. The uncertainty distributions obtained for the effective homogeneous material configuration were clearly less scattered than those obtained for the bimaterial configuration and were included in their $[25th, 75th]$ percentile ranges (not shown here). This was a direct consequence of the lower level of the uncertainties of the effective hydraulic properties of the material compared to those of compost and pozzolan.

The means of these uncertainty distributions for each time point, simulation configurations and depths are also presented in Figs. 8. The curves obtained for the effective homogeneous material and the explicit two-component medium were similar. This con-

firms the validity of the upscaling approach in our study. However, some discrepancies appeared as simulation time increased. Table 4 shows the mean water matric potential values and the mean water content values for both configurations at $t_{max} = 10$ days, the final time point of the evaporation simulation. Table 4 shows the water matric potential means for each depth, and taking into account all of the uncertainties. Relative differences between the bimaterial configuration and the corresponding effective homogeneous material configuration were relatively high for water matric potentials, and were more pronounced in-depth. However, these relative differences concerned an area of the core where the porous media were quite dry. Water content values of both the bimaterial and the homogeneous material configurations were computed from these water matric potentials using the van-Genutchen model and the parameters estimated for the effective material configuration given in Table 2. These water content values presented in Table 4 show only slight differences between the two configurations, and the relative differences (between 2.1% and 6.4% at 10 days) are lower than those of the water matric potentials.

Discrepancies may be due to the non-equilibrium flow process, a consequence of the occurrence of transient processes during the dynamic simulation. Results obtained by *Šimůnek et al.* [2001] showed that modeling a non-equilibrium flow modifies the dynamic response for infiltration scenarios, but hardly affects the dynamic response for evaporation scenarios. During the evaporation simulation, the average macroscopic flux was a vertical upward flux. However, the orientation of the local, microscopic water flux could be derived from the vertical direction, due to the presence of local heterogeneous water potential gradients as shown in Figs. 7. The tortuosity of the water flow was, thus, increased. This local tortuosity is a kind of balance between the boundary conditions

leading to a vertical macroscopic flux and the contrast of the hydraulic properties of both materials leading to the multidimensionnal microscopic water flux. The contrast of the hydraulic properties depends on the local water content or matric potentials, and as these variables were time dependent during the dynamic simulation, the tortuosity was also time dependent. This time-dependent tortuosity was not accounted for during the upscaling process since the determination of the effective properties was performed under successive states of equilibrium, see section 3.2. As a consequence of this time dependency of the local tortuosity, the overall evaporation process of the heterogeneous medium could be accelerated or slowed down compared to the effective material. Therefore, more complex models including non-equilibrum terms might be implemented to study their influence on the dynamic response using the present configuration.

5. Conclusion

The hydraulic properties of a heteregeneous medium were studied at the Darcy scale using two different approaches. The first methodological approach consisted in determining the water retention and hydraulic conductivity curves for the components of the heteregeneous medium. The material considered herein was a green roof substrate, which is a composite of compressible materials, bark compost, and of aggregates of volcanic rock, pozzolan. Associated uncertainties were evaluated using a boostrap method. It was shown, on a virtual evaporation experiment, that the impact of these uncertainties on the simulated water matric potential was high.

The second methodological approach consisted in considering the heterogeneous medium as an homogeneous material using an upscaling method. Effective water retention and hydraulic conductivity curves were fitted on values computed for several water matric po-

tentials using numerical steady-state scenarios on the considered heterogenous material. Associated uncertainties of these properties were also evaluated taking into account the uncertainties of the hydraulic properties of the components of the heterogeneous material. To that effect, for each hydraulic property, N couples of curves were sampled in the uncertainty distributions of the components in an independent way for a set of water matric potential values. N was set at a high value, and the water matric potential values were optimally chosen. We have shown, here, that this methodology led to very low levels of uncertainties in the effective properties of the material. A direct consequence of this approach was that the uncertainties of simulated water potential for the effective homogeneous material were very low compared to those obtained on the equivalent heterogeneous material. This has shown that the use of effective properties for a heterogenous material reduced the impact of the uncertainties in the properties of its components. This is of importance since the uncertainties linked to the experimental disposal and to the variability of the materials properties may be high, as shown in the first part of the study. It must be noted that the level of uncertainty obtained here for the simulation of water matric potential in the effective material under evaporation conditions is not representative of the level of uncertainty expected on the simulation of a real evaporation experiment. In this last case, other types of uncertainties, such as uncertainties on initial and boundary conditions for example, must be taken into account.

Although the level of uncertainties obtained on the simulations of the water matric potential differed for the heterogeneous and effective materials, their mean values were almost similar. This confirms the adequacy of the upscaling approach, for the heterogeneous material and associated configuration, used in this study. The slight discrepancies

observed between these means may be due to the absence of non-equilibrium term in the simulation model used. This term could be included in the scope of future studies.

Acknowledgments.

This work was supported by the French National Research Agency (ANR) through the "Habitat intelligent et solaire photovoltaique" program (project AGROBAT ANR-09-HABISOL-001). We also thank the CINES (Centre Informatique National de l'Enseignement Supérieur, France) for offering us access to the supercomputer JADE to conduct these calculations successfully. The authors wish to thank Profs. L. Di Pietro, G. Micolau, H. Bolvin and Dr. C. Doussan for their helpful comments and careful readings of the manuscript.

References

Renard, Ph., G. de Marsily (1997), Calculating equivalent permeability: a review, *Adv Water Resour, 20(5-6)*, 253–278.

Feyen, J., D. Jacques, A. Timmerman, J. Vanderborght (1998), Modelling water flow and solute transport in heterogeneous soils: a review of recent approaches, *J Agric Eng Res, 70(3)*, 231–256.

Vogel H.J., K. Roth (2003), Moving through scales of flow and transport in soil, *J Hydrol, 272(1-4)*, 95–106.

Vereecken H., R. Kasteel, J. Vanderborght, T. Harter (2007), Upscaling hydraulic properties and soil water flow processes in heterogeneous soils: a review, *Vadose Zone J, 6*, 1–28.

Vogel H.J., U. Weller, O. Ippisch (2010), Non-equilibrium in soil hydraulic modelling, *J Hydrol, 393(1-2)*, 20–28.

Samouëlian A., I. Cousin, C. Dagès, A. Frison, G. Richard (2011), Determining the effective hydraulic properties of a highly heterogeneous soil horizon, *Vadose Zone J, 10(1)*, 450–458.

Ma D., M. Shao, J. Zhang, Q. Wang (2010), Validation of an analytical method for determining soil hydraulic properties of stony soils using experimental data, *Geoderma, 159*, 262–269.

Danquigny C., P. Ackerer (2005), Experimental determination of equivalent parameters of a heterogeneous porous medium under uniform or radial flow, *CR Geosci, 337(6)*, 563–570.

Samouëlian A., H.J. Vogel, O. Ippisch (2007), Upscaling hydraulic conductivity based on the topology of the sub-scale structure, *Adv Water Resour, 30(5)*, 1179–1189.

Vogel H.J., K. Roth (1998), A new approach for determining soil hydraulic functions, *Eur J Soil Sci, 49(4)*, 547–556.

Javaux M., M. Vanclooster (2006), Three-dimensional structure characterisation and transient flow modelling of a variably saturated heterogeneous monolith, *J Hydrol, 327(3-4)*, 516–524.

Mohrath D., L. Bruckler, P. Bertuzzi, J.C. Gaudu, M. Bourlet (1967), Error analysis of an evaporation method for determining hydrodynamic properties in unsaturated soil, *Soil Sci Soc Am J, 61(3)*, 725–735.

Peters A., W. Durner (2008), Simplified evaporation method for determining soil hydraulic properties, *J Hydrol, 356(1-2)*, 147–162.

Christiaens K., J. Feyen (2001), Analysis of uncertainties associated with different methods to determine soil hydraulic properties and their propagation in the distributed hydrological MIKE SHE model, *J Hydrol, 246(1-4)*, 63–81.

Coppola A., A. Basile, A. Comegna, N. Lamaddalena (2009), Monte Carlo analysis of field water flow comparing uni- and bimodal effective hydraulic parameters for structured soil, *J Contam Hydrol, 104(1-4)*, 153–165.

Pan F., M. Ye, J. Zhu, Y.S. Wu, B.X. Hu, Z. Yu (2009), Numerical evaluation of uncertainty in water retention parameters and effect on predictive uncertainty, *Vadose Zone J, 8(1)*, 158–166.

Efron B., R. Tibshirani (1993), An Introduction to the Bootstrap, *Boca Raton, FL: Chapman & Hall/CRC Monographs on Statistics & Applied Probability.*

Manly B.F.J. (2007), Randomization, Bootstrap and Monte Carlo Methods in Biology, *Boca Raton, FL: Chapman & Hall/CRC.*

Vogel H.J., A. Samouëlian, O. Ippisch (2008), Multi-step and two-step experiments in heterogeneous porous media to evaluate the relevance of dynamic effectes, *Adv Water Resour, 31(1)*, 181–188.

Šimůnek J., O. Wendroth, N. Wypler, Mth. van Genuchten (2001), Non-equilibrium water flow characterized by means of upward infiltration experiments, *Eur J Soil Sci, 52(1)*, 13–24.

Anonymous. (2002), www.fll.de. Guidelines for the planning, execution and upkeeping of green-roof sites, *Bonn:FLL Ed.*

Tamari S., L. Bruckler, J. Halbertsma, J. Chadoeuf (1993), A simple method for determining soil hydraulic properties in the laboratory, *Soil Sci Soc Am J, 57(3)*, 642–651.

Dane J.H., J.W. Hopmans (2002), Method of Soil analysis - Part 4 Physical Method, *In: Dane JH, Topp GC, editors. Water retention and storage, Madison:SSSA book series.*

Monnier G., P. Stengel, J.C. Fiès (1973), Une méthode de mesure de la densité apparente de petits agglomérats terreux. Application à l'analyse des systèmes de porosité du sol, *In: Annales Agronomiques.*

van Genuchten MTh. (1980), A closed-form equation for predicting the hydraulic conductivity of unsaturated soils, *Soil Sci Soc Am J, 44(5)*, 892–898.

Coleman T.F., Y. Li (1996), An Interior, Trust Region Approach for Nonlinear Minimization Subject to Bounds, *SIAM J Optim, (6)*, 418–445.

Chossat J.C. (2005), La mesure de la conductivité hydraulique dans les sols - Choix des méthodes, *Paris:Tec et Doc Ed - Lavoisier.*

Kutilek M., D.R. Nielsen (1994), Soil Hydrology, *Catena Verlag.*

Celia M.A., E.T. Bouloutas, R.L. Zarba (1990), A general mass-conservative numerical solution for the unsaturated flow equation, *Water Resour Res, 26(7)*, 1483–1496.

Kavetski D., P. Binning, S.W. Sloan (2001), Adaptive time stepping and error control in a mass conservative numerical solution of the mixed form of Richards equation, *Adv Water Resour, 24(6)*, 595–605.

Renaud J., H. Cloke, Y. Wang, M. Anderson, P. Wilkinson, D. Lloyd (2003), Simulation numérique d'écoulements en milieu poreux avec l'équation de Richards, *Eur J Comput Mech, 12(2-3)*, 203–220.

Dhatt G., G. Touzot, E. Lefrancois (1984), Méthode des éléments finis, *London:Hermes Science Publications - Lavoisier.*

727 Ju S.H., K.J.S. Kung (1997), Mass types, element orders and solution schemes for the
728 Richards equation, *Comput Geosci, 23(2)*, 175–187.

729 Huang K., B.P. Mohanty, Mth. van Genuchten (1996), A new convergence criterion for
730 the modified Picard iteration method to solve the variably saturated flow equation, *J*
731 *Hydrol, 178(1-4)*, 69–91.

732 Fityus S.G., D.W. Smith (2001), Solution of the unsaturated soil moisture equation using
733 repeated transforms, *Int J Numer Anal Methods Geomech, 25(15)*, 1501–1524.

734 Tracy F.T. (2007), Three-dimensional analytical solutions of Richards' equation for a
735 box-shaped soil sample with piecewise-constant head boundary conditions on the top,
736 *J Hydrol, 336(3-4)*, 391–400.

737 Vanderborght J., R. Kasteel, M. Herbst, M. Javaux, D. Thiéry, M. Vanclooster, C. Mou-
738 vet, H. Vereecken (2005), A set of analytical benchmarks to test numerical models of
739 flow and transport in soils, *Vadose Zone J, 4(1)*, 206–221.

740 Hardelauf H., M. Javaux, M. Herbst, S. Gottschalk, R. Kasteel, J. Vanderborght, H.
741 Vereecken (2007), PARSWMS: A parallelized model for simulating three-dimensional
742 water flow and solute transport in variably saturated soils, *Vadose Zone J, 6(2)*, 255–
743 259.

744 Herbst M., S. Gottschalk, M. Reissel, H. Hardelauf, R. Kasteel, M. Javaux, J. Vander-
745 borght, H. Vereecken (2008), On preconditioning for a parallel solution of the Richards
746 equation, *Comput Geosci, 34(12)*, 1958–1963.

747 Atkinson A.C., A.N. Donev (1992), Optimum experimental designs, *Oxford:Clarendon*
748 *Press.*

749 Dexter A.R., E.A. Czyz, G. Richard, A. Reszkowska (2008), A user-friendly water re-
750 tention function that takes account of the textural and structural pore spaces in soil,
751 *Geoderma, 143(3-4)*, 243–253.

752 Hopmans J.W., J. Šimůnek, N. Romane, W. Durner (2002), Method of Soil analysis -
753 Part 4 Physical Method, *In: Dane JH, Topp GC editors. Simultaneous determination*
754 *of water transmission and retention properties - Inverse methods, Madison:SSSA book*
755 *series.*

756 Matheron G. (1967), Eléments pour une Théorie des Milieux Poreux, *Paris:Masson et*
757 *Cie.*

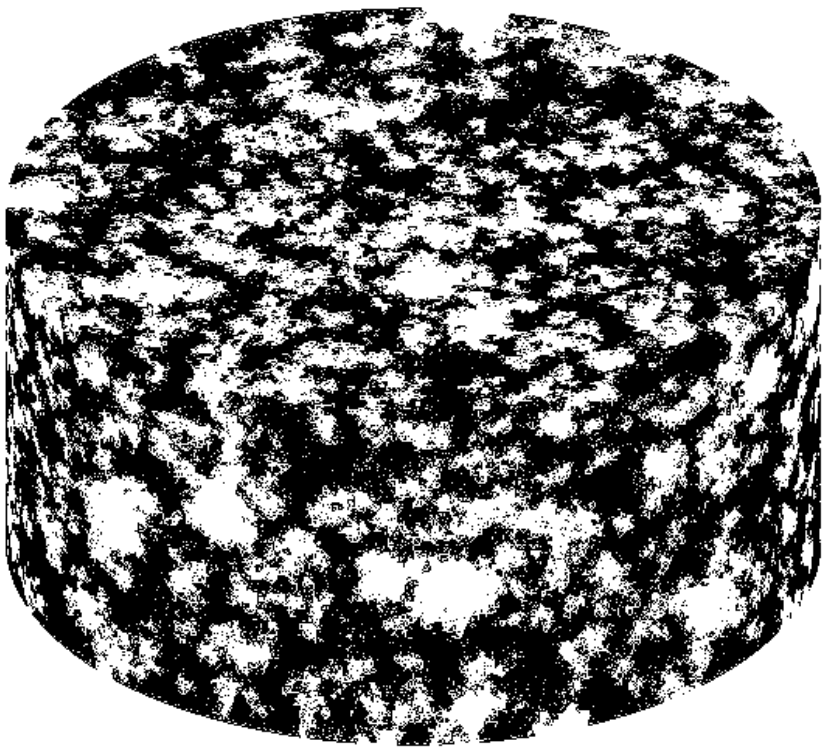

Figure 1. Typical heteregeneous mesh for the bimaterial configuration. Black or white zones correspond, respectively, to the pozzolan or bark compost component.

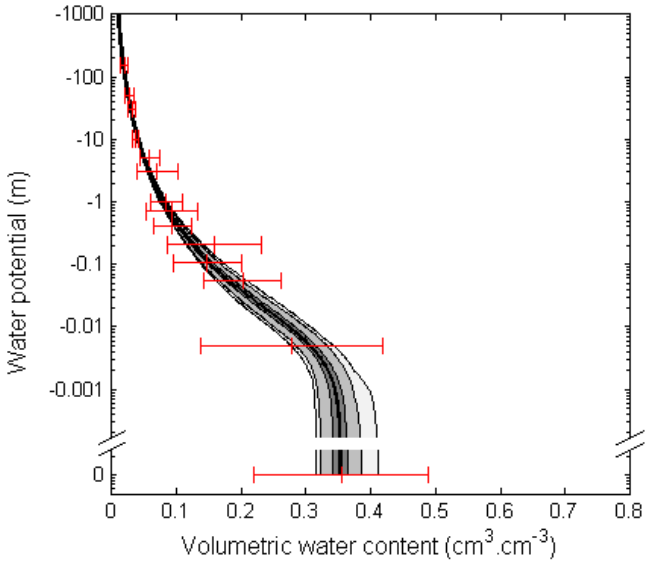

(a)

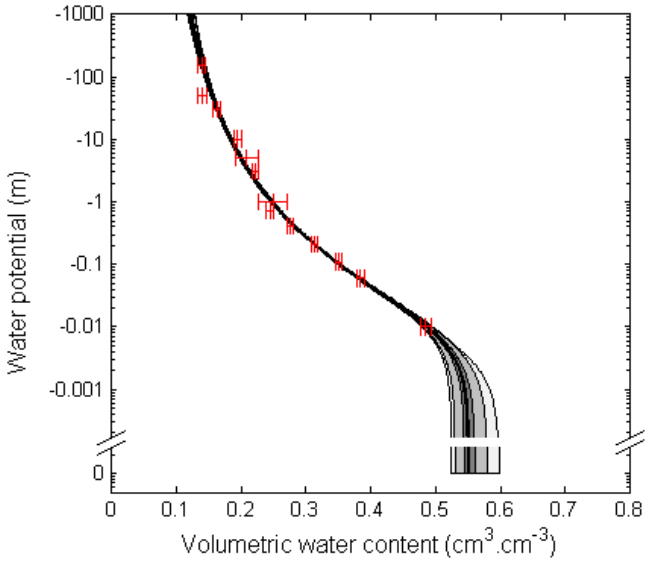

(b)

Figure 2. Uncertainty distributions of a) pozzolan and b) compost water retention values. Crosses and error bars represent means and ± 1 standard deviations of measured data and curves represent $0.5, 2.5, 25, 75, 97.5, 99.5$ percentiles and median of the estimated water retention uncertainty distributions. Vertical axes are in log scale.

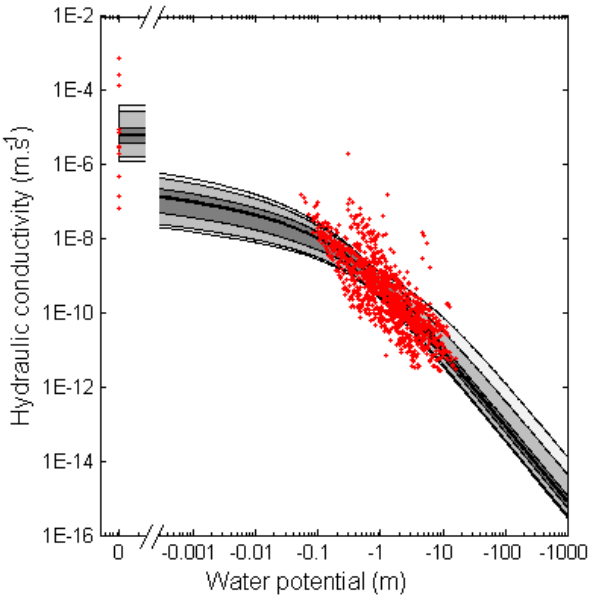

(a)

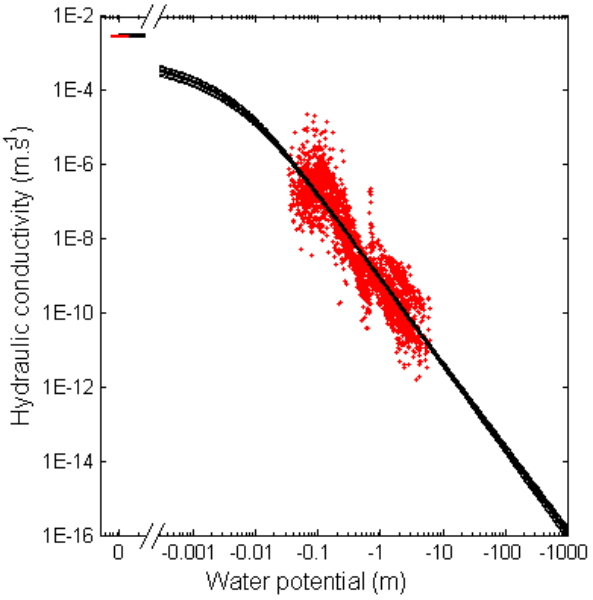

(b)

Figure 3. Uncertainty distributions of a) pozzolan and b) compost hydraulic conductivity values. Crosses represent measured data and curves represent $0.5, 2.5, 25, 75, 97.5, 99.5$ percentiles and median of the estimated hydraulic conductivity distributions. Vertical and horizontal axes are in log scale.

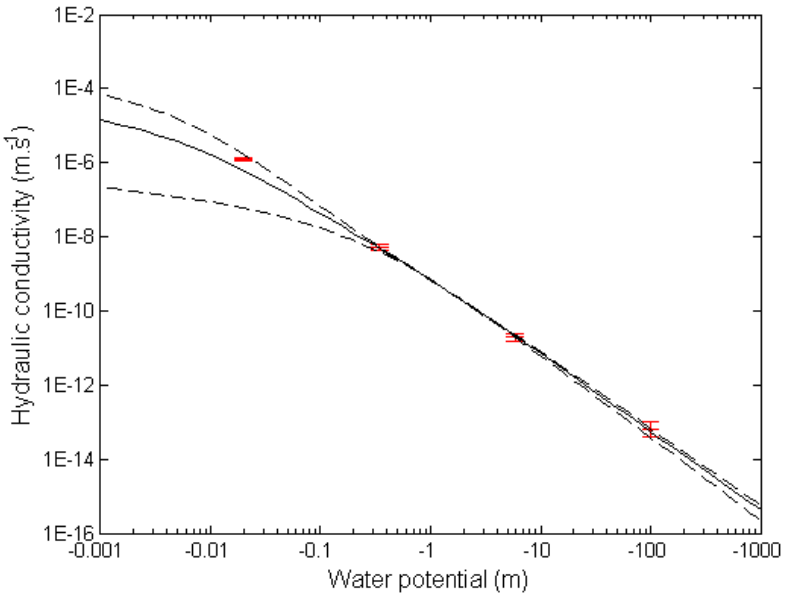

(a)

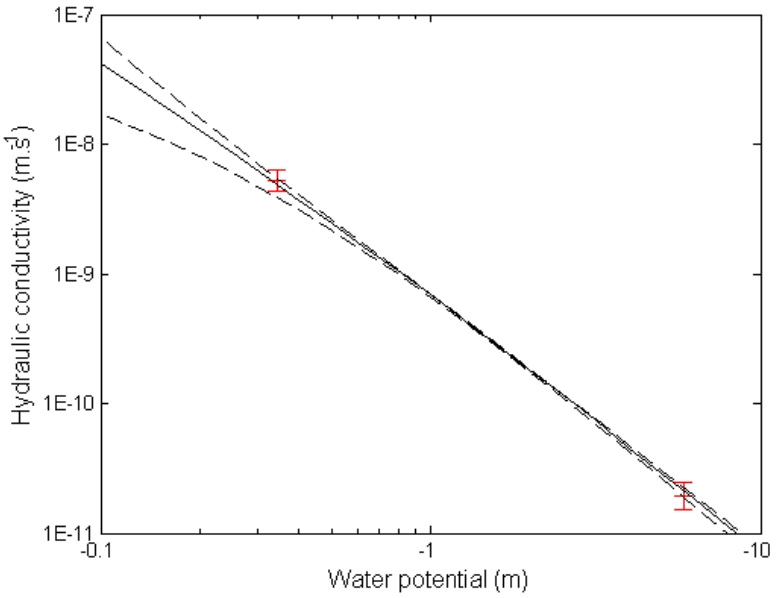

(b)

Figure 4. Effective conductivity values computed from 200 compost and pozzolan properties for 4 water matric potential values. Crosses represent the mean and ±1 standard deviations of the 50 computed values per water matric potential point, dotted lines are the means of the Wiener bounds and the plain line is the Matheron curve obtained from these mean curves. Fig. b) is an enhanced view of Fig. a). Vertical and horizontal axes are in log scale.

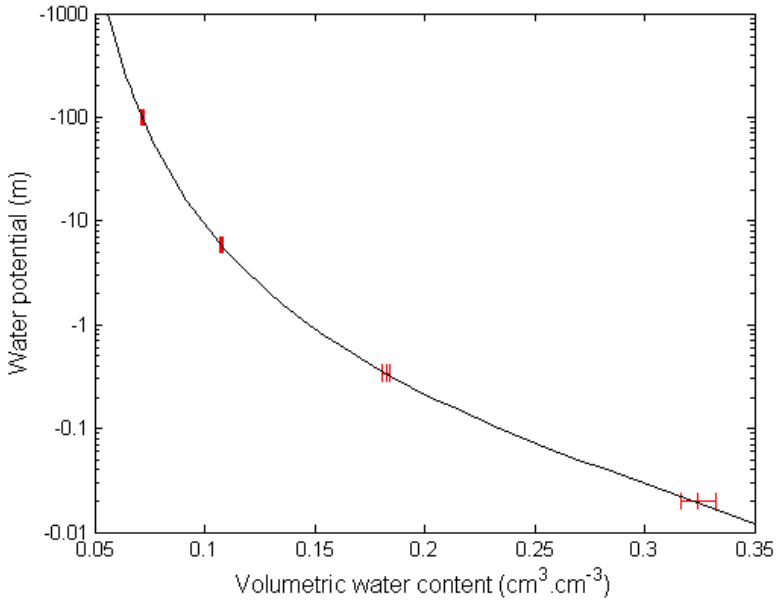

Figure 5. Effective retention values computed from 200 compost and pozzolan properties for 4 water matric potential values. Crosses represent the mean and ±1 standard deviations of the 50 computed values per water matric potential point and the plain line is the mean of the arithmetic mean curves obtained from the compost and pozzolan retention curves used. The horizontal axis is in log scale.

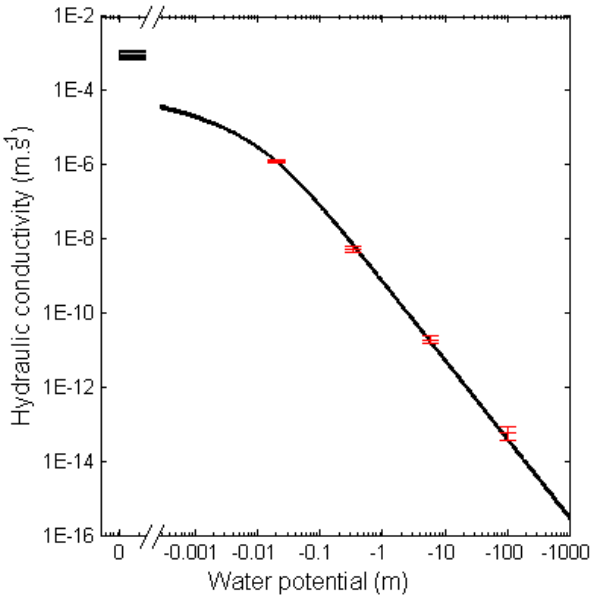

(a)

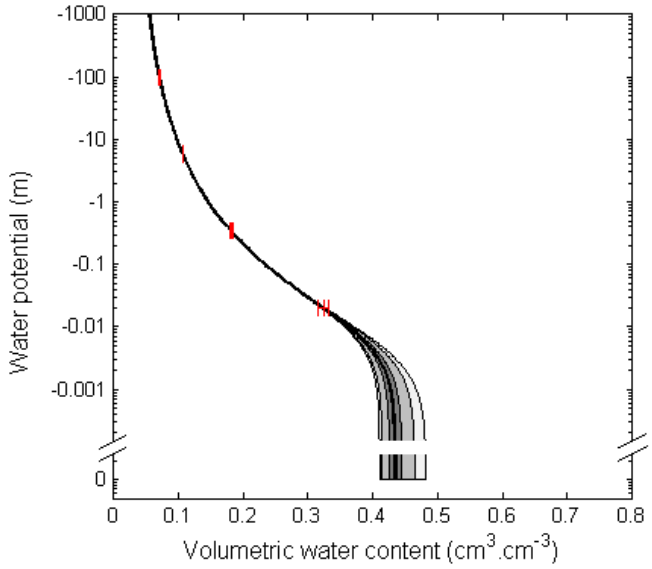

(b)

Figure 6. Uncertainty distributions of a) effective hydraulic conductivity and b) water retention. Crosses and error bars represent means and ± 1 standard deviations of simulated data and curves represent $0.5, 2.5, 25, 75, 97.5, 99.5$ percentiles and median of the estimated hydraulic conductivity and water retention distributions. The vertical axes are in log scale. The horizontal axis of plot a) is also in log scale.

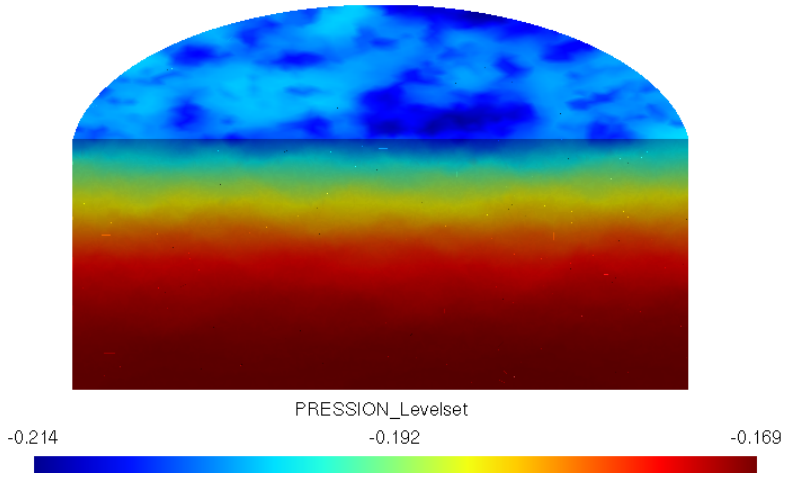

(a)

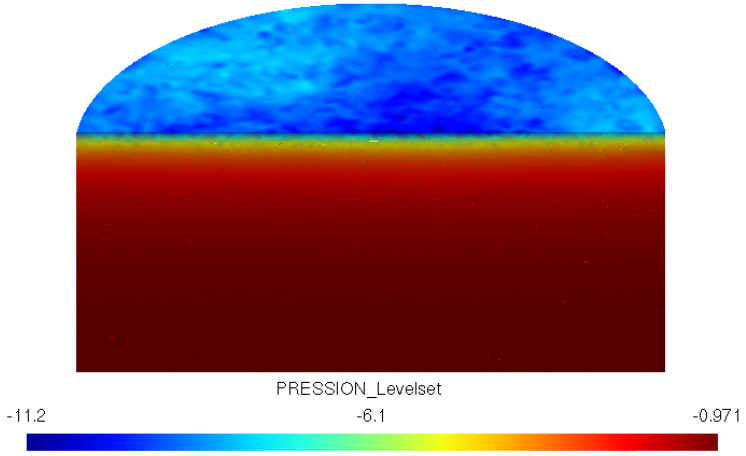

(b)

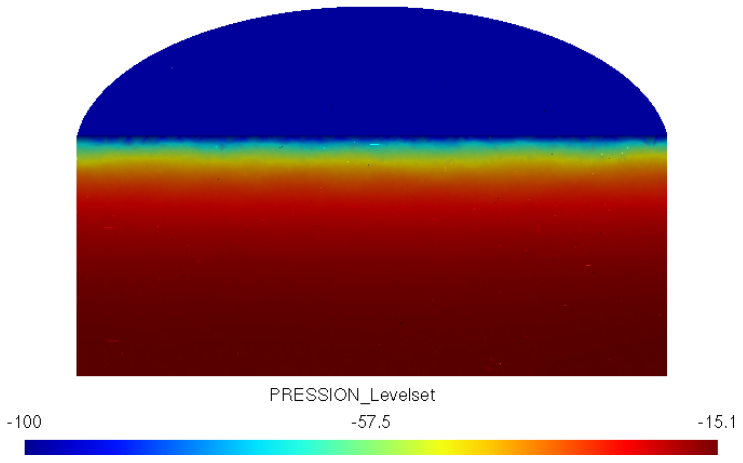

(c)

Figure 7. Snapshots of the evolution of the water potential according to time, at a) $t = 2$ days, b) $t = 6$ days and c) $t = 10$ days. Scales for water matric potential are different for each snapshot.

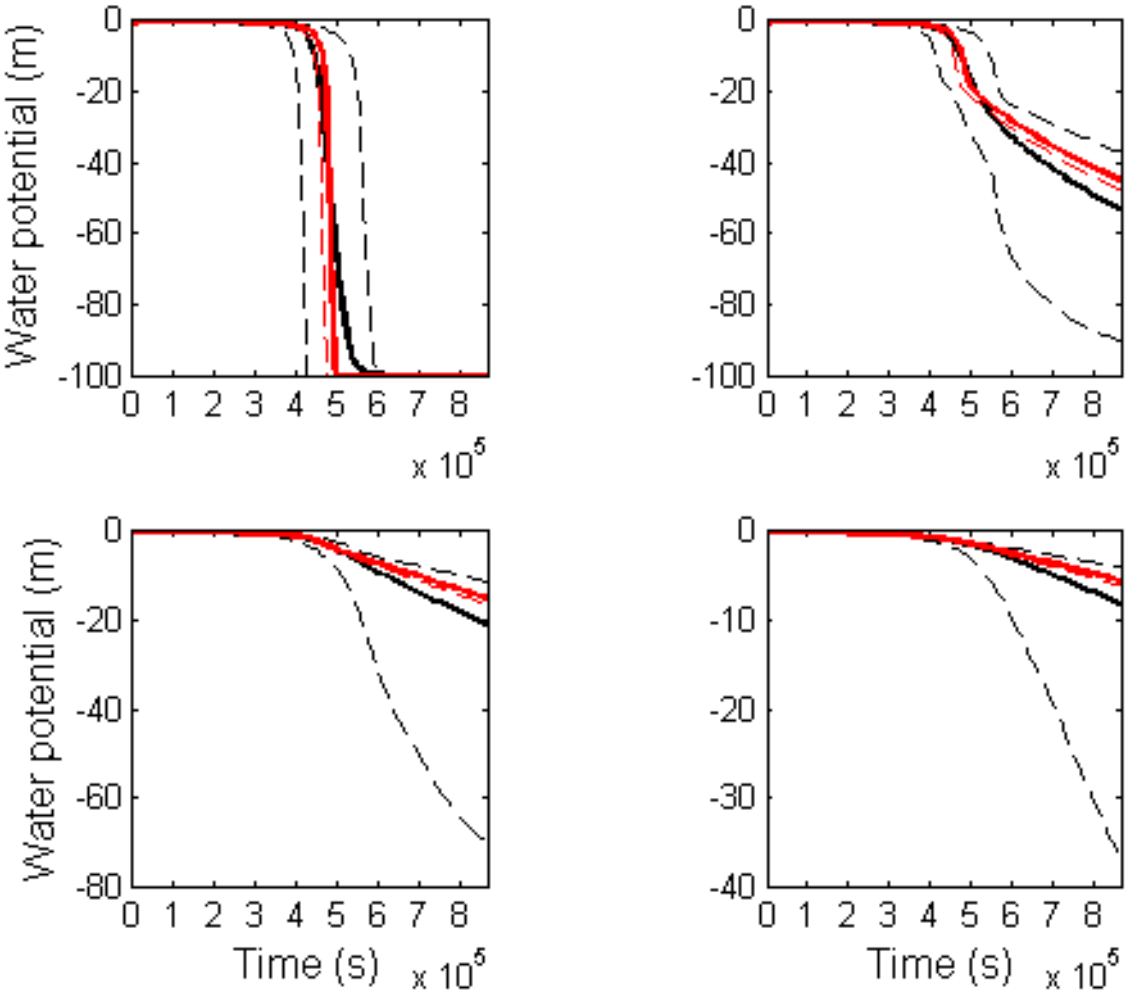

Figure 8. Uncertainty distributions of water matric potential values obtained by simulating evaporation using the heterogeneous green roof substrate (black curves) and using the corresponding computed effective homogeneous material (red curves). Dotted or solid curves represent, respectively, $0.5, 99.5$ percentile or median values for the water matric potential distributions. The 4 graphs correspond to 4 various depths of the core.

		Pozzolan aggregate	Complex substrate	Bark compost
Particle density	Mean	3.000	-	1.670
	σ coefficient of variation	0.020 0.7%	- -	0.040 2.4%
Apparent bulk density	Mean	1.520	0.822	0.195
	σ coefficient of variation	0.230 15.1%	0.002 0.2%	0.003 1.5%

Table 1. Mean and standard deviation values of the particle and apparent bulk densities for bark compost, pozzolan aggregate and complex substrate.

		θ_r	θ_s	h_e	n
Compost	Estimat. value	$8.66e^{-2}$	$5.55e^{-1}$	$7.47e^{-3}$	1.22
	σ	$5.92e^{-3}$ (6.9%)	$1.27e^{-2}$ (2.3%)	$1.63e^{-3}$ (21.8%)	$1.01e^{-2}$ (0.8%)
Pozzolan	Estimat. value	$0(fixed)$	$3.53e^{-1}$	$5.88e^{-3}$	1.29
	σ	$0(fixed)$	$1.63e^{-2}$ (4.6%)	$2.05e^{-3}$ (34.9%)	$1.11e^{-2}$ (0.9%)
Effective material	Estimat. value	$3.81e^{-2}$	$4.35e^{-1}$	$6.71e^{-3}$	1.26
	σ	$7.17e^{-4}$ (1.9%)	$1.36e^{-2}$ (3.1%)	$1.04e^{-3}$ (15.5%)	$2.74e^{-3}$ (0.2%)

Table 2. Estimated values and associated uncertainties of the van Genuchten model parameters for water retention of compost, pozzolan and effective material.

		K_{Sat}	h_e	n
Compost	Estimat. value	$3.04e^{-3}$	$9.72e^{-3}$	1.12
	σ	$1.03e^{-4}$ (3.4%)	$2.79e^{-4}$ (2.9%)	$8.87e^{-3}$ (0.8%)
Pozzolan	Estimat. value	$6.94e^{-6}$	$6.01e^{-1}$	1.02
	σ	$7.95e^{-6}$ (114.6%)	$9.90e^{-1}$ (164.7%)	$9.64e^{-3}$ (0.9%)
Effective material	Estimat. value	$9.36e^{-4}$	$2.28e^{-2}$	1.05
	σ	$8.91e^{-5}$ (9.5%)	$8.01e^{-4}$ (3.5%)	$1.91e^{-3}$ (0.2%)

Table 3. Estimated values and associated uncertainties of the Mualem-van Genuchten model parameters for hydraulic conductivity of compost, pozzolan and effective material.

		Depth= -0.2 cm	Depth= -1.1 cm	Depth= -4.8 cm
Water matric potential means	Effective homogeneous material configuration	-45.78	-15.33	-5.68
	Bimaterial configuration	-53.71	-21.47	-8.36
	Relative differences	14.8%	28.6%	32.1%
Water content means	Effective homogeneous material configuration	7.81 e-2	9.12 e-2	10.69 e-2
	Bimaterial configuration	7.65 e-2	8.68 e-2	10.00 e-2
	Relative differences	2.1%	4.9%	6.4%

Table 4. Means of all water matric potential and water content values for several depth and for the bimaterial and effective material configurations.